Classification of guided wave propagation in a cylindrical pipe and verification by the finite element method

Harumichi Sato† (AIST)

1. Introduction

Cylindrical pipes are widely used in various industrial applications, rendering their nondestructive inspection crucial to meet standard or regulatory requirements. Guided wave propagation is a very promising method for inspecting cylindrical pipes nondestructively and in short time, and propagation in hollow pipes has already been investigated theoretically by Gazis.[1] The author classified guided waves as longitudinal mode (L-mode), flexural mode (F-mode), and torsional mode (T-mode), of which only the F-mode was found dependent on the circumferential parameter ($n > 0$), as opposed to the L- and T-modes ($n = 0$) which did not. Furthermore, Nishino *et al.* the dispersion curves of guided waves and proposed that the n-parameter of the T-mode was not limited to zero.[2] The author investigated the dispersion curves of guided waves and showed that the T-mode could not be clearly separated from the F-mode for $n > 0$.[3] In this article, we further theoretical results, which are then verified by the finite element method (FEM).

2 Theoretical results

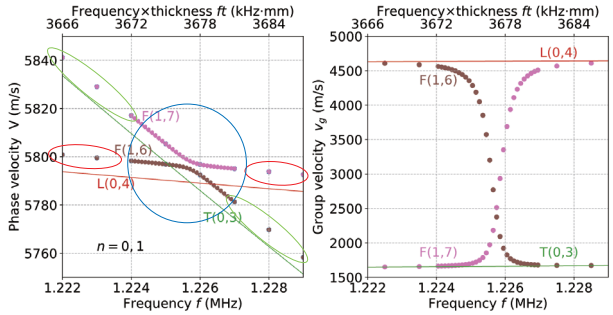

Fig. 1. Phase and group velocities of L(0,4), T(0,3), F(1,6), and F(1,7)

Fig. 1 demonstrates the phase (Fig. 1a) and group velocities (Fig. 1b) of L(0,4), T(0,3), F(1,6), and F(1,7) of guided waves propagating in a pipe whose outer and inner diameters are $\phi 34$ mm and $\phi 28$ mm, respectively, and its sound velocities of longitudinal and transverse waves are 5790 m/s and 3100 m/s, respectively. Fig. 1a shows that L(0,4) and T(0,3) intersect near 1.226 MHz, whereas F(1,6) and F(1,7) do not intersect at any frequency. It is also shown that is impossible to separate the higher order T-modes (with $n > 0$) from the F-modes (F(1,6) or F(1,7)). In Fig. 1a, guided waves surrounded by two red circles are considered as F-modes, those surrounded by two green circles are considered as the higher order T-modes, and those surrounded by one blue circle are considered as the mixture modes. Furthermore, Fig. 1b reveals that group velocity varies considerably in the mode mixture area.

3 Finite element method and results

An FEM solver with cylindrical coordinates was developed and used to simulate guided waves propagating in a pipe. The model was based on a pipe whose diameters were the same as those found by the theoretical analysis and whose length was 1000 mm. The $z = 0$ and $z = 1000$ mm surfaces were set as the periodic boundary conditions. The sound velocities of the longitudinal and transverse waves were the same as those of the theoretical analysis, and the density was 7910 kg/m^3. The model was divided by the eight-node hexahedral elements shown in Fig. 2a, and the surface set as the force boundary condition was divided by the four-node quadrilateral elements shown in Fig.3a. These shapes are presented in local coordinate systems in Figs. 2b and 3b. The interpolation functions were defined as follows:

$$N_i(\xi,\eta,\zeta) = \frac{1}{8}(1+\xi\xi_i)(1+\eta\eta_i)(1+\zeta\zeta_i), \quad i = 1\text{–}8$$

$$N_i^s(\xi,\eta) = \frac{1}{4}(1+\xi\xi_i)(1+\eta\eta_i), i = 1\text{–}4 \quad .$$

The size of the hexahedral elements is $\Delta r = \Delta z = 0.25$ mm, $\Delta\theta = \pi/212$ and the size of the quadrilateral elements is $\Delta r = \Delta z = 0.25$ mm.

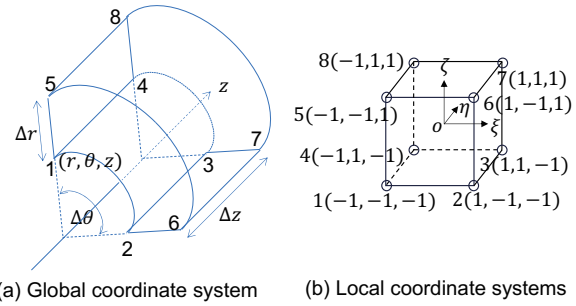

(a) Global coordinate system (b) Local coordinate systems

Fig. 2. Eight-node hexahedral element

We then used an explicit method in the solver. The finite element formulation for time transit problem was expressed by the following equation[4]

$$[M]\{\ddot{u}\} + [K]\{u\} = \{F\} \quad ,$$

where $[M]$ is the mass matrix, $[K]$ is the stiffness matrix, $\{u\}$ is the nodal displacement vector, and ·

E-mail: †h.sato@aist.go.jp

denotes the time derivative. Entries of $[K]$ were expressed as follows:

$$[K] = \sum_{e=1}^{n} \int_{v^e} [B]^T [D][B] dv \quad ,$$

where $\Sigma_{e=1}^{n}$ expresses the summation of all elements and $[D]$ is the elastic stiffness matrix. Displacements in the $r, \theta,$ and z coordinates were expressed as $u_r, u_\theta,$ and u_z, respectively. In addition, we know that the strain tensor in the cylindrical coordinates is defined by the equations below.

$$\varepsilon_{rr} = \frac{\partial u_r}{\partial r}, \varepsilon_{\theta\theta} = \frac{1}{r}\frac{\partial u_\theta}{\partial \theta} + \frac{u_r}{r}, \varepsilon_{zz} = \frac{\partial u_z}{\partial z},$$
$$2\varepsilon_{rz} = \frac{\partial u_r}{\partial z} + \frac{\partial u_z}{\partial r}, 2\varepsilon_{r\theta} = \frac{1}{r}\frac{\partial u_r}{\partial \theta} + \frac{\partial u_\theta}{\partial r} - \frac{u_\theta}{r},$$
$$2\varepsilon_{\theta z} = \frac{\partial u_\theta}{\partial z} + \frac{1}{r}\frac{\partial u_z}{\partial \theta} \quad .$$

$[B]$ is determined by the strain tensor, and in this case it is a 6×24 matrix,

$$[B] = \begin{bmatrix} \frac{\partial N_1}{\partial r} & 0 & 0 & \frac{\partial N_2}{\partial r} \\ \frac{N_1}{r} & \frac{1}{r}\frac{\partial N_1}{\partial \sigma} & 0 & \frac{N_2}{r} \\ 0 & 0 & \frac{\partial N_1}{\partial z} & 0 \\ 0 & \frac{\partial N_1}{\partial z} & \frac{1}{r}\frac{\partial N_1}{\partial \theta} & 0 \\ \frac{\partial N_1}{\partial z} & 0 & \frac{\partial N_1}{\partial r} & \frac{\partial N_2}{\partial z} \\ \frac{1}{r}\frac{\partial N_1}{\partial \theta} & \frac{\partial N_1}{\partial r} - \frac{N_1}{r} & 0 & \frac{1}{r}\frac{\partial N_2}{\partial \theta} \end{bmatrix}$$
$$\begin{matrix} \cdots & 0 & 0 & \frac{\partial N_8}{\partial r} & 0 & 0 \\ \cdots & \frac{1}{r}\frac{\partial N_7}{\partial \sigma} & 0 & \frac{N_8}{r} & \frac{1}{r}\frac{\partial N_8}{\partial \sigma} & 0 \\ \cdots & 0 & \frac{\partial N_7}{\partial z} & 0 & 0 & \frac{\partial N_8}{\partial z} \\ \cdots & \frac{\partial N_7}{\partial z} & \frac{1}{r}\frac{\partial N_7}{\partial \theta} & 0 & \frac{\partial N_8}{\partial z} & \frac{1}{r}\frac{\partial N_8}{\partial \theta} \\ \cdots & 0 & \frac{\partial N_7}{\partial r} & \frac{\partial N_8}{\partial z} & 0 & \frac{\partial N_8}{\partial r} \\ \cdots & \frac{\partial N_7}{\partial r} - \frac{N_7}{r} & 0 & \frac{1}{r}\frac{\partial N_8}{\partial \theta} & \frac{\partial N_8}{\partial r} - \frac{N_8}{r} & 0 \end{matrix} \Bigg].$$

Moreover, the entries of $\{F\}$ were expressed by the following equation

$$\{F\} = \sum_{e \in S_\sigma} \int_{s_\sigma e} [N]^T \{\bar{T}\} ds \quad ,$$

where $\Sigma_{e \in S_\sigma}$ expresses the summation of all boundary integrals, $\{\bar{T}\}$ is the force boundary condition, and $[N]$ is a 3×12 matrix whose entries are shown below:

$$[N] = \begin{bmatrix} N_1^S & 0 & 0 & N_2^S & \cdots & 0 & 0 \\ 0 & N_1^S & 0 & 0 & \cdots & N_4^S & 0 \\ 0 & 0 & N_1^S & 0 & \cdots & 0 & N_4^S \end{bmatrix}.$$

To generate guided waves, the force boundary condition simulated the phase velocity scanning method[5, 6] was set on the surface of the model:

$$\{\bar{T}\}^T = (0 \quad 0 \quad T_3)$$

$$T_3 = A_3 \exp\left\{-\frac{(t-t_0)^2}{2c_2^2}\right\} \exp\left\{-\frac{(z-z_0)^2}{2c_1^2}\right\} \times \cos n\theta \sin\left\{2\pi f\left(t - \frac{z-z_0}{v}\right)\right\}$$

using the following parameters:

$A_3 = 1.0$ MPa, $f = 1.2257$ MHz, $v = 5794.9$ m/s, $z_0 = 43$ mm, $t_0 = 7.35$ μs, $c_1 = 10.0$ mm, $c_2 = 1.73$ μs, and $n = 1$.

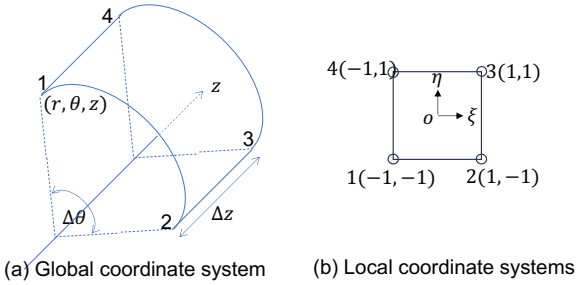

(a) Global coordinate system (b) Local coordinate systems

Fig. 3. Four-node quadrilateral element

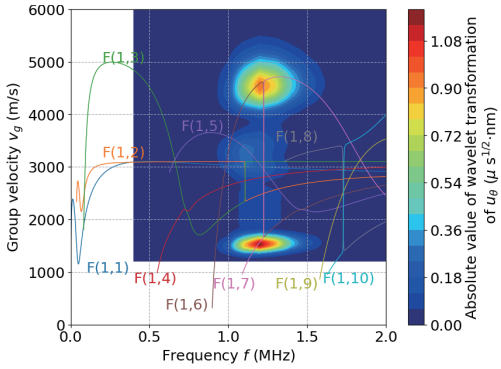

Fig. 4. Group velocity and result of FEM.

Fig. 4 shows the group velocities obtained by the theoretical analysis (represented by curves) and the FEM result (represented by the contour map). It can be seen that the group velocities of F(1,2), F(1,3), F(1,8), and F(1,10) also vary considerably in the mode mixture areas. The contour map is a wavelet transform of u_θ at $z = 250$ mm and $\theta = \pi/2$. The FEM result is in good agreement with the theoretical results. Consequently, we consider that the theoretical result is reliable and the Gazis's classification is more acceptable.

Acknowledgments

This work was supported by JSPS KAKENHI Grant Number JP26390109. The author would like to thank Enago (www.enago.jp) for the English language review.

References

1) D. C. Gazis, Jpn. J. Acoust. Soc. Am. **31**, 568 (1959).
2) H. Nishino *et al.*, Jpn. J. Appl. Phys. **40**, 364 (2001).
3) H. Sato, Proc. 43rd Symp. Ultrasonic Electronics, 2022, 3Pa2-9.
4) M. Yagawa and S. Yoshimura, Yugenyosoho (Finite element method) (Baifukan, Tokyo, 1991) p. 171 [in Japanese].
5) K. Yamanaka *et al.*, Appl. Phys. Lett. **58**, 1591 (1991).
6) H. Nishino *et al.*, Appl. Phys. Lett. **62**, 2036 (1993).